Paraxial propagation along the optical axis of a uniaxial medium

Alessandro Ciattoni*
Dipartimento di Fisica, Università Roma Tre, I-00146 Rome, Italy
and Istituto Nazionale di Fisica della Materia Unità di Roma 3, Rome, Italy

Gabriella Cincotti and Damiano Provenziani
Dipartimento di Ingegneria Elettronica, Università Roma Tre, I-00146 Rome, Italy
and Istituto Nazionale di Fisica della Materia Unità di Roma 3, Rome, Italy

Claudio Palma
Dipartimento di Fisica, Università Roma Tre, I-00146 Rome, Italy
and Istituto Nazionale di Fisica della Materia Unità di Roma 3, Rome, Italy
(Received 29 April 2002; published 24 September 2002)

An approach for describing paraxial propagation of light along the optical axis of a uniaxial medium is introduced. Contrary to previous theoretical schemes, our approach directly deals with the propagation of the whole optical field without resorting to the standard decomposition into ordinary and extraordinary parts, thus avoiding some related mathematical difficulties. A paraxial equation governing the field propagation has been derived, and its formal solution has been deduced. The structure of this solution allows us to think of the optical field in the crystal as the corresponding one propagating in vacuum ''dressed'' by the effect of anisotropy. This relationship is used to derive two analytical techniques for evaluating the propagated field. Starting from the formal solution, the closed-form expression of the anisotropic propagator is also derived. The proposed approach is used to predict the evolution of an astigmatic Gaussian beam through a calcite crystal, which has been also experimentally investigated. The agreement between theory and experiment is good.

DOI: 10.1103/PhysRevE.66.036614 PACS number(s): 42.25.Bs, 41.20.Jb

I. INTRODUCTION

Optical propagation inside anisotropic media is a subject still receiving a good deal of attention, mainly because of its intrinsic vectorial features [1–3]. Among the classical topics, the transmission and reflection of light at the interface between an isotropic and an anisotropic medium [4–7] and the propagation through birefringent optical fibers [8] have been largely investigated during past decades. The most intriguing influence a crystal exhibits on light propagation consists in inducing a change in the polarization state of the incoming radiation [9,10]. In fact, the vast majority of devices based on anisotropic materials is devoted to produce light with a desired polarization state [11–13]. Light propagation through these devices is usually described by means of theoretical approaches representing the light as a plane wave, so that the whole realm of diffractive phenomena is generally neglected. This description is accurate enough whenever the beam waist is much greater than the wavelength, but this condition is not always fulfilled in actual experiments, where the beams are often micronsized or smaller. This justifies the demand of a paraxial theory of propagation, dealing with optical beams and not with plane waves only. Besides, it is also conceptually intriguing to investigate the propagation of beams undergoing both diffraction and depolarization at the same time, since their simultaneous occurrence generates nontrivial polarization patterns and field distribution.

Various approaches dealing with propagation of beams in uniaxially anisotropic media have been proposed. For instance, Stamnes *et al.* [14] employ of a plane-wave angular spectrum representation in order to predict the field radiated by a finite source inside an unbounded uniaxial crystal, under very general conditions (nonmonochromatic fields, dispersive materials and arbitrary propagation direction). The only shortcoming of this approach resides in the inherent mathematical complexity. Fleck *et al.* [15] give approximate paraxial equations for both the ordinary and the extraordinary components of the field, even though the boundary field decomposition into ordinary and extraordinary components is not immediate. Trippenbach *et al.* [16–19] consider the propagation of light pulses in nonisotropic and dispersive media, deriving the equation for the slowly varying envelope of the electric field. Recently, a different theoretical scheme has been proposed [20], where the exact plane-wave angular spectrum representation has been approximated within the paraxial constraint, obtaining the paraxial expressions for the ordinary and extraordinary components of a field propagating along the optical axis. In that approach the authors also describe the way to extract the ordinary and the extraordinary parts from the boundary field, but, unfortunately, this decomposition is not mathematically simple.

Generally speaking, almost all the approaches presented in literature share a common logical path. First, the boundary field is represented as a superposition of an ordinary and extraordinary components; then it is shown that these two fields propagate independently because the ordinary and extraordinary plane waves are eigenwaves of the Maxwell equations; the propagated field is finally obtained as the superposition of the propagated ordinary and extraordinary

*Electronic address: ciattoni@fis.uniroma3.it

components, exploiting the intrinsic linearity of the propagation process. Although this is the most natural way of reasoning, there are reasons suggesting that a description of propagation of the global optical field would be better in some cases. First of all, such a description would avoid the analytical difficulties associated with the ordinary-extraordinary decomposition. Second from an experimental point of view, the Cartesian field components can be directly measured, whereas the ordinary and extraordinary entities are not easy to separate.

In the present paper, the formalism of Ref. [20] is exploited to develop an innovative scheme for describing paraxial propagation of light along the optical axis of a uniaxial crystal, without resorting to the usual ordinary-extraordinary decomposition of the field. Basically, we derive two coupled paraxial equations governing the evolution of the transverse Cartesian components of the field. Their coupling reflects the simple fact that the polarization state of the radiation traveling in the crystal generally changes; besides, it is responsible for an energy exchange between the Cartesian components [21].

One of the major virtues of these equations is that they are much simpler to tackle numerically than the integral expressions for the ordinary and extraordinary fields. Besides, their structure reveals that the field propagating in the crystal can be thought of as a field propagating in vacuum with the same boundary distribution, affected by an anisotropic perturbation. This observation offers a further way of understanding the propagation process and a consequent deeper physical insight; this connection has been already pointed out for the particular case of cylindrically symmetric fields [22].

The solution of the new propagation equations can be formally written and manipulated in order to get some interesting general consequences. First, we elucidate rigorously and in a simple way, the connection existing between the field in the crystal and the corresponding field in the vacuum. In fact, in the proposed solution, it is possible to keep the effect of the anisotropy apart from the isotropic diffractive dynamics; thus the field propagating in the crystal naturally appears as the corresponding one propagating in vacuum ''dressed'' by the effect of the anisotropy.

As a straightforward application, we develop two different analytical techniques for evaluating the field in the crystal: the first one is a convenient mathematical restatement of the above-mentioned connection, and the second one is a perturbation scheme exploiting the paraxiality of the field in vacuum.

Another general consequence of the scheme comes out from the fact that the proposed solution formally links the field at any transverse plane to the boundary field at the entrance facet of the crystal. This allows us to explain the propagation process as a linear system and to give the expression of the paraxial anisotropic propagator.

As a test, we finally investigate the propagation of an astigmatic Gaussian beam along the optical axis of a calcite crystal. The case does not admit a fully analytical treatment because of the complexity of the involved integrals. On the other side, the propagation of an astigmatic Gaussian beam in vacuum has a closed form expression, so that it is appealing to be investigated by means of our techniques. For this aim, we employ the perturbation scheme, which is particularly useful for longitudinal propagation distances of about of a few diffraction lengths. Moreover, we employ a suitable numerical algorithm in order to deal with the formal expression of the propagated field.

Finally, we experimentally investigate the propagation of an astigmatic Gaussian beam in a calcite crystal: the agreement between theoretical predictions and experimental results is good.

II. PROPAGATION EQUATION FOR THE PARAXIAL FIELD

Let us consider a homogeneous nonabsorbing uniaxial crystal whose dielectric tensor is

$$\epsilon = \begin{pmatrix} n_o^2 & 0 & 0 \\ 0 & n_o^2 & 0 \\ 0 & 0 & n_e^2 \end{pmatrix}, \tag{1}$$

where n_o and n_e are the ordinary and extraordinary refractive indices, respectively. Propagation of a paraxial beam along the optical axis has been investigated in Ref. [20], where it is shown that the slowly varying amplitude $\mathbf{A}_\perp$ of the transverse part of the field $\mathbf{E}_\perp = E_x\hat{\mathbf{e}}_x + E_y\hat{\mathbf{e}}_y = \exp(ik_0 n_o z)\mathbf{A}_\perp$ ($k_0 = \omega/c$ being the wave number in vacuum) is given by $\mathbf{A}_\perp = \mathbf{A}_{\perp o} + \mathbf{A}_{\perp e}$, where

$$\mathbf{A}_{\perp o}(\mathbf{r}_\perp, z) = \int d^2\mathbf{k}_\perp e^{i\mathbf{k}_\perp\cdot\mathbf{r}_\perp} e^{-(iz/2k_0 n_o)k_\perp^2} \times \frac{1}{k_\perp^2}\begin{pmatrix} k_y^2 & -k_x k_y \\ -k_x k_y & k_x^2 \end{pmatrix} \tilde{\mathbf{A}}_\perp(\mathbf{k}_\perp),$$

$$\mathbf{A}_{\perp e}(\mathbf{r}_\perp, z) = \int d^2\mathbf{k}_\perp e^{i\mathbf{k}_\perp\cdot\mathbf{r}_\perp} e^{-(in_o z/2k_0 n_e^2)k_\perp^2} \times \frac{1}{k_\perp^2}\begin{pmatrix} k_x^2 & k_x k_y \\ k_x k_y & k_y^2 \end{pmatrix} \tilde{\mathbf{A}}_\perp(\mathbf{k}_\perp), \tag{2}$$

are the slowly varying amplitudes of the ordinary and extraordinary contributions to the field, respectively. Here $\mathbf{r}_\perp = x\hat{\mathbf{e}}_x + y\hat{\mathbf{e}}_y$, $\mathbf{k}_\perp = k_x\hat{\mathbf{e}}_x + k_y\hat{\mathbf{e}}_y$, whereas the vectorial angular spectrum $\tilde{\mathbf{A}}$ is the two-dimensional Fourier transform of the transverse field at $z=0$,

$$\tilde{\mathbf{A}}_\perp(\mathbf{k}_\perp) = \frac{1}{(2\pi)^2}\int d^2\mathbf{r}_\perp e^{-i\mathbf{k}_\perp\cdot\mathbf{r}_\perp}\mathbf{E}_\perp(\mathbf{r}_\perp, 0). \tag{3}$$

Equations (2) and (3) allow us to evaluate the field in the crystal when it is known on the plane $z=0$. In order to get a picture of propagation not based on the ordinary-extraordinary decomposition, we focus our attention on the whole field $\mathbf{A}_\perp$ and we start by noting that, from Eqs. (2), it is

$$i\frac{\partial \mathbf{A}_\perp}{\partial z}+\frac{1}{2k_0n_o}\nabla_\perp^2\mathbf{A}_\perp = \frac{\Delta}{2k_0n_o}\int d^2\mathbf{k}_\perp e^{i\mathbf{k}_\perp\cdot\mathbf{r}_\perp}e^{-(in_oz/2k_0n_e^2)k_\perp^2} \times\begin{pmatrix} k_x^2 & k_xk_y \\ k_xk_y & k_y^2\end{pmatrix}\tilde{\mathbf{A}}_\perp(\mathbf{k}_\perp), \quad (4)$$

where $\nabla_\perp^2=\partial_x^2+\partial_y^2$ and $\Delta=n_o^2/n_e^2-1$ is a parameter associated with the degree of anisotropy of the medium. However, it is rather simple to show that

$$\hat{\mathbf{T}}\cdot\mathbf{A}_\perp\equiv\begin{pmatrix}\partial_x^2 & \partial_{xy}^2\\ \partial_{xy}^2 & \partial_y^2\end{pmatrix}\mathbf{A}_\perp = -\int d^2\mathbf{k}_\perp e^{i\mathbf{k}_\perp\cdot\mathbf{r}_\perp}e^{-(in_oz/2k_0n_e^2)k_\perp^2}\begin{pmatrix} k_x^2 & k_xk_y \\ k_xk_y & k_y^2\end{pmatrix} \times\tilde{\mathbf{A}}_\perp(\mathbf{k}_\perp), \quad (5)$$

which, combined with Eq. (4), gives

$$i\frac{\partial \mathbf{A}_\perp}{\partial z}+\frac{1}{2k_0n_o}\nabla_\perp^2\mathbf{A}_\perp=-\frac{\Delta}{2k_0n_o}\hat{\mathbf{T}}\cdot\mathbf{A}_\perp. \quad (6)$$

Equation (6) furnishes an alternative paraxial approach to propagation in uniaxial crystal, which is equivalent to that offered by the explicit expressions of Eqs. (2). In fact, it can be shown that the field $\mathbf{A}_{\perp o}+\mathbf{A}_{\perp e}$ of Eqs. (2) is the unique solution of Eq. (6) satisfying the boundary condition $\mathbf{E}_\perp(\mathbf{r}_\perp,0)$. Equation (6) can be seen as the anisotropic counterpart of the parabolic equation describing paraxial propagation in homogeneous isotropic media, to which it reduces in the isotropic limit (i.e., $n_o=n_e=n$ or $\Delta=0$).

The structure of Eq. (6) suggests a different way to figure light propagation through an anisotropic medium. The key observation is that the *whole* effect of the anisotropy is embedded in the right-hand side of Eq. (6), while the left-hand side is identical to that of the paraxial equation for an isotropic medium of refractive index n_o. This means that there must be a way of keeping the isotropic diffraction and the anisotropic influence apart. More pictorially, this allows us to view the field propagating in the crystal as a field propagating in the isotropic medium *warped* by the anisotropy.

Splitting Eq. (6) into its two Cartesian components, we get

$$i\frac{\partial A_x}{\partial z}+\frac{1}{2k_0n_o}\left(\frac{n_o^2}{n_e^2}\frac{\partial^2}{\partial x^2}+\frac{\partial^2}{\partial y^2}\right)A_x=-\frac{\Delta}{2k_0n_o}\frac{\partial^2A_y}{\partial x\partial y},$$

$$i\frac{\partial A_y}{\partial z}+\frac{1}{2k_0n_o}\left(\frac{\partial^2}{\partial x^2}+\frac{n_o^2}{n_e^2}\frac{\partial^2}{\partial y^2}\right)A_y=-\frac{\Delta}{2k_0n_o}\frac{\partial^2A_x}{\partial x\partial y}. \quad (7)$$

We observe that the equations governing the evolution of the Cartesian components A_x and A_y are *coupled* as a consequence of the anisotropy, Δ playing the role of a *coupling constant*, as intuitively expected. The major consequences are that the state of polarization of the beam generally changes during propagation and that a power exchange between the two components takes place [21]. From a physical point of view, such a coupling can be understood by noting that the ordinary and extraordinary fields show different diffraction behaviors, since the quadratic terms $k_\perp^2$ in the exponentials of Eqs. (2) are multiplied by different coefficients and Δ is proportional to their difference. Therefore, the two fields mutually slide, preventing the polarization state at $z=0$ to be reconstructed for $z>0$, since the ordinary and extraordinary polarization patterns are generally nontrivial [see Eqs. (2)]. This polarization dynamics can be figured out as a coupling between the two components, and it is also very intuitive that its strength is proportional to the anisotropy parameter Δ.

A reader can notice a similarity between Eq. (7) and the differential equations of Ref. [16]. In that paper, Trippenbach *et al.* consider a very general case of propagation of light pulses through noninsotropic and dispersive media, but the comprehension of the evolution of the polarization state is not immediate.

III. CONSEQUENCES OF THE PROPAGATION EQUATION

Although equivalent in describing paraxial propagation, the approaches based on the angular spectrum representation of Eqs. (2) and on the propagation equation Eq. (6), are somehow complementary. In fact, Eqs. (2) are physically intuitive and simple enough to give a sufficient understanding of propagation, and of a number of its features [23–25]. Nevertheless, performing the integrals is generally a difficult task in practical situations, because of the highly oscillatory behavior of the integrands; in this perspective, Eq. (6) is much more suitable for numerical computations, because of its simple structure. Besides, Eq. (6) simply yields some general results concerning propagation, whose deduction from the angular spectrum approach is lengthy and not physically enlightening.

The starting point consists in noting that the formal solution of Eq. (6) with the boundary condition $\mathbf{E}_\perp(\mathbf{r}_\perp,0)$ is given by

$$\mathbf{A}_\perp(\mathbf{r}_\perp,z)=e^{(iz\Delta/2k_0n_o)\hat{\mathbf{T}}}e^{(iz/2k_0n_o)\nabla_\perp^2}\mathbf{E}_\perp(\mathbf{r}_\perp,0), \quad (8)$$

as it can be straightforwardly verified; here the exponentials are defined by the usual power-series definition of a function of operator [i.e., $\exp(\hat{\mathbf{O}})=\Sigma_{n=0}^{\infty}\hat{\mathbf{O}}^n/n!$]. Note that the operators $\nabla_\perp^2$ and $\hat{\mathbf{T}}$ commute (i.e., $\nabla_\perp^2\hat{\mathbf{T}}=\hat{\mathbf{T}}\nabla_\perp^2$) so that they can be treated as c numbers in formal manipulations. Equation (8) is an elegant way of expressing the field inside the crystal, the price of this compactness is the formality of handling functions of operators.

A. Connection between the field in the crystal and in vacuum

One of the most intriguing point suggested by the proposed approach is that the paraxial field propagating in the crystal is closely related to the corresponding one propagating in vacuum. As noticed in the preceding section, anisotropy can be viewed as a perturbation to isotropic diffraction and their effects can be separately taken into account, because of the linearity of the propagation process. In order to convert this observation into a mathematical expression, we introduce the field

$$\mathbf{A}_\perp^{(0)}(\mathbf{r}_\perp,z)=e^{(iz/2k_0)\nabla_\perp^2}\mathbf{E}_\perp(\mathbf{r}_\perp,0), \tag{9}$$

which coincides with $\mathbf{E}_\perp(\mathbf{r}_\perp,0)$ on the plane $z=0$ and satisfies the parabolic equation

$$i\frac{\partial\mathbf{A}_\perp^{(0)}}{\partial z}+\frac{1}{2k_0}\nabla_\perp^2\mathbf{A}_\perp^{(0)}=0. \tag{10}$$

$\mathbf{A}_\perp^{(0)}$ describes the paraxial field propagating in vacuum with the same boundary distribution of $\mathbf{A}_\perp$. Equation (8) can be rewritten as

$$\mathbf{A}_\perp(\mathbf{r}_\perp,z)=e^{(iz\Delta/2k_0n_o)\hat{\mathbf{T}}}\mathbf{A}_\perp^{(0)}\left(\mathbf{r}_\perp,\frac{z}{n_0}\right)\equiv\hat{\mathbf{D}}(z)\mathbf{A}_\perp^{(0)}\left(\mathbf{r}_\perp,\frac{z}{n_0}\right), \tag{11}$$

which establishes the desired connection between $\mathbf{A}_\perp$ and $\mathbf{A}_\perp^{(0)}$. Equation (11) is very interesting from both a conceptual and an analytical point of view. In fact, it allows us to figure the field in the crystal as the *bare* field propagating in vacuum *dressed* by the action of the anisotropic operator $\hat{\mathbf{D}}$. Moreover Eq. (11) shows that it is possible to take the effect of the anisotropy into account after the simpler associated isotropic problem has been solved.

By exploiting the properties of the operator $\hat{\mathbf{T}}$ we give a less formal aspect to Eq. (11); in fact, the effect of the operator $\hat{\mathbf{D}}$ can be worked out, giving (see part A of the Appendix)

$$\mathbf{A}_\perp(\mathbf{r}_\perp,z)=\begin{pmatrix}\partial_y^2 & -\partial_{xy}^2\\ -\partial_{xy}^2 & \partial_x^2\end{pmatrix}\mathbf{F}_\perp\left(\mathbf{r}_\perp,\frac{z}{n_o}\right)+\begin{pmatrix}\partial_x^2 & \partial_{xy}^2\\ \partial_{xy}^2 & \partial_y^2\end{pmatrix}\mathbf{F}_\perp\left(\mathbf{r}_\perp,\frac{n_0z}{n_e^2}\right), \tag{12}$$

where the field

$$\mathbf{F}_\perp(\mathbf{r}_\perp,z)=\frac{1}{2\pi}\int d^2\mathbf{r}'_\perp\ln|\mathbf{r}_\perp-\mathbf{r}'_\perp|\mathbf{A}_\perp^{(0)}(\mathbf{r}'_\perp,z) \tag{13}$$

has been introduced. Equation (12) represents an alternative advantageous way for evaluating the field inside an anisotropic medium: if the vacuum field $\mathbf{A}_\perp^{(0)}$ is known, the difficulty of determining the field in the crystal is reduced to the evaluation of the field $\mathbf{F}_\perp$ in Eq. (13), since $\mathbf{A}_\perp$ descends from it by means of simple spatial differentiations. Note that the two contributions in the right-hand side of Eq. (12) are the the ordinary and extraordinary fields, respectively: they are both generated by the field $\mathbf{F}_\perp$, enlightening their common origin.

Equation (11) is also suitable for a perturbation scheme to evaluate the field at some distances from the plane $z=0$. By using the power-series definition of the exponential, from Eq. (11), we have

$$\mathbf{A}_\perp(\mathbf{r}_\perp,z)=\left[1+\frac{iz\Delta}{2k_0n_o}\hat{\mathbf{T}}\sum_{n=1}^{\infty}\frac{1}{n!}\left(\frac{iz\Delta}{2k_0n_o}\nabla_\perp^2\right)^{n-1}\right]\times\mathbf{A}_\perp^{(0)}\left(\mathbf{r}_\perp,\frac{z}{n_0}\right), \tag{14}$$

where use has been made of the relation $\hat{\mathbf{T}}^n=\hat{\mathbf{T}}(\nabla_\perp^2)^{n-1}$, derived in part A of the Appendix. The series in the right-hand side of this equation is highly oscillating for large z; this is not a serious shortcoming as actual crystals are generally not very long. Besides, there are two physical reasons to employ Eq. (14): first, the majority of the crystals is slightly anisotropic (n_o and n_e are very close) so that Δ is always smaller than 1 (as an example, for the calcite it is $\Delta\simeq0.24$). In second place, the field $\mathbf{A}_\perp^{(0)}$ is slowly varying as a paraxial field, that is to say $|(\nabla_\perp^2)^{n+1}\mathbf{A}_\perp^{(0)}(\mathbf{r}_\perp,z)|\ll|(\nabla_\perp^2)^n\mathbf{A}_\perp^{(0)}(\mathbf{r}_\perp,z)|$. This allows us to truncate the series up to the first order, that is,

$$\mathbf{A}_\perp(\mathbf{r}_\perp,z)=\left[1+\frac{iz\Delta}{2k_0n_o}\hat{\mathbf{T}}\left(1+\frac{iz\Delta}{4k_0n_o}\nabla_\perp^2\right)\right]\mathbf{A}_\perp^{(0)}\left(\mathbf{r}_\perp,\frac{z}{n_0}\right). \tag{15}$$

In order to obtain the longitudinal distances z for which this relation holds, it is sufficient to assure that the neglected second-order term is much smaller than the first-order one. Since it is $\nabla_\perp^2\mathbf{A}_\perp^{(0)}\sim k_0^2f^2\mathbf{A}_\perp^{(0)}$, where $f=\lambda/w$ is the degree of paraxially of $\mathbf{A}_\perp^{(0)}$ (w measuring the waist of the beam and λ the vacuum wavelength), it is simple to show that Eq. (15) is valid for $z<z_M=6n_o/(k_0f^2\Delta)$ which, for paraxial beams is generally comparable with the size of actual crystals. The proposed perturbation scheme is very handy, because all the required contributions can be obtained from the vacuum field $\mathbf{A}_\perp^{(0)}$ by means of spatial differentiations only.

B. Anisotropic propagators

Another remarkable property of Eq. (8) is that it embodies a direct relation between the boundary field $\mathbf{E}_\perp(\mathbf{r}_\perp,0)$ and the propagated one $\mathbf{A}_\perp(\mathbf{r}_\perp,z)$. Such a way of understanding propagation is very common in optics, as the propagation process can be viewed as a linear system and the output field is obtained by convolving the input one with a propagator. In order to obtain the propagator for an anisotropic medium, let us rewrite Eq. (8) as

$$\mathbf{A}_\perp(\mathbf{r}_\perp,z)=\int d^2\mathbf{r}'_\perp[e^{(iz\Delta/2k_0n_o)\hat{\mathbf{T}}}e^{(iz/2k_0n_o)\nabla_\perp^2}\delta(\mathbf{r}_\perp-\mathbf{r}'_\perp)]\times\mathbf{E}_\perp(\mathbf{r}'_\perp,0)\equiv\int d^2\mathbf{r}'_\perp\mathbf{G}(\mathbf{r}_\perp-\mathbf{r}'_\perp)\mathbf{E}_\perp(\mathbf{r}'_\perp,0),\tag{16}$$

where the convolution property of the Dirac delta function $\delta(\mathbf{r}_\perp-\mathbf{r}'_\perp)$ has been exploited. This equation shows that the anisotropic exponential operator in Eq. (8) is an integral operator whose kernel $\mathbf{G}(\mathbf{r}_\perp-\mathbf{r}'_\perp)$ is the desired anisotropic propagator. Inserting the well-known integral representation of the Dirac delta function into the definition of $\mathbf{G}(\mathbf{r}_\perp-\mathbf{r}'_\perp)$ and exploiting Eq. (A3) of part A of the Appendix, we straightforwardly obtain

$$\mathbf{G}(\mathbf{r}_\perp-\mathbf{r}'_\perp)=\frac{1}{(2\pi)^2}\int d^2\mathbf{k}_\perp(\nabla_\perp^2)^{-1}[(\nabla_\perp^2-\hat{\mathbf{T}})e^{(iz/2k_0n_o)\nabla_\perp^2}+\hat{\mathbf{T}}e^{(in_oz/2k_0n_e^2)\nabla_\perp^2}]e^{i\mathbf{k}_\perp\cdot(\mathbf{r}_\perp-\mathbf{r}'_\perp)}.\tag{17}$$

Note that the plane waves $\exp(i\mathbf{k}_\perp\cdot\mathbf{r}_\perp)$ are eigenfunctions of both $\hat{\mathbf{T}}$ and $\nabla_\perp^2$, so that Eq. (17) can be rewritten as

$$\mathbf{G}(\mathbf{r}_\perp-\mathbf{r}'_\perp)=\int\frac{d^2\mathbf{k}_\perp}{(2\pi)^2}e^{i\mathbf{k}_\perp\cdot(\mathbf{r}_\perp-\mathbf{r}'_\perp)-(iz/2k_0n_o)k_\perp^2}\frac{1}{k_\perp^2}\times\begin{pmatrix}k_y^2 & -k_xk_y\\ -k_xk_y & k_x^2\end{pmatrix}+\int\frac{d^2\mathbf{k}_\perp}{(2\pi)^2}e^{i\mathbf{k}_\perp\cdot(\mathbf{r}_\perp-\mathbf{r}'_\perp)-(in_oz/2k_0n_e^2)k_\perp^2}\frac{1}{k_\perp^2}\times\begin{pmatrix}k_x^2 & k_xk_y\\ k_xk_y & k_y^2\end{pmatrix}\equiv\mathbf{G}_o(\mathbf{r}_\perp-\mathbf{r}'_\perp)+\mathbf{G}_e(\mathbf{r}_\perp-\mathbf{r}'_\perp),\tag{18}$$

where each operator has been replaced with the corresponding eigenvalue. Equation (18) reveals that the anisotropic propagator is the sum of an ordinary and an extraordinary contribution, $\mathbf{G}_o$ and $\mathbf{G}_e$, respectively, restating the well-known physical fact that these two field independently propagate [see Eqs. (2)]. The integrals in Eq. (18) can be analytically performed (see part B of the Appendix), yielding

$$\mathbf{G}_o(\mathbf{R})=\frac{k_0n_o}{4\pi iz}e^{-(k_0n_o/2iz)R^2}\begin{pmatrix}1 & 0\\ 0 & 1\end{pmatrix}-\left[\frac{k_0n_o}{4\pi iz}e^{-(k_0n_o/2iz)R^2}-\frac{1-e^{-(k_0n_o/2iz)R^2}}{2\pi R^2}\right]\frac{1}{R^2}\begin{pmatrix}X^2-Y^2 & 2XY\\ 2XY & -X^2+Y^2\end{pmatrix},$$

$$\mathbf{G}_e(\mathbf{R})=\frac{k_0n_e^2}{4\pi in_oz}e^{-(k_0n_e^2/2in_oz)R^2}\begin{pmatrix}1 & 0\\ 0 & 1\end{pmatrix}+\left[\frac{k_0n_e^2}{4\pi in_oz}e^{-(k_0n_e^2/2in_oz)R^2}-\frac{1-e^{-(k_0n_e^2/2in_oz)R^2}}{2\pi R^2}\right]\frac{1}{R^2}\begin{pmatrix}X^2-Y^2 & 2XY\\ 2XY & -X^2+Y^2\end{pmatrix},\tag{19}$$

where we set $\mathbf{R}=X\hat{\mathbf{e}}_x+Y\hat{\mathbf{e}}_y=\mathbf{r}_\perp-\mathbf{r}'_\perp$, for the sake of simplicity. Note that the description of propagation in uniaxial media by means of propagators has been investigated in Ref. [3], where integral expressions for the exact propagators are given. It is remarkable that, within the paraxial approximation, the propagators are expressed in a closed form.

Both the propagators $\mathbf{G}_o$ and $\mathbf{G}_e$ are the sum of an isotropic Fresnel-like term and an anisotropic one. Note that in the isotropic limit $n_o=n_e=n$ the anisotropic terms compensate each other, giving

$$\mathbf{G}(\mathbf{R})=\mathbf{G}_o(\mathbf{R})+\mathbf{G}_e(\mathbf{R})=\frac{k_0n}{2\pi iz}e^{-(k_0n/2iz)R^2},\tag{20}$$

which, as expected, coincides with the well-known Fresnel propagator for an homogeneous and isotropic medium of refractive index n [26].

IV. THE ASTIGMATIC GAUSSIAN BEAM

Let us consider the propagation of a paraxial beam whose boundary distribution is given by

$$\mathbf{E}_\perp(\mathbf{r}_\perp,0)=E_0e^{-(x^2/2s_x^2)-(y^2/2s_y^2)}\hat{\mathbf{e}}_x,\tag{21}$$

that is to say an astigmatic Gaussian beam characterized by two variances s_x^2 and s_y^2, a unique waist plane, and a linear polarization along the x axis. In this case, Eq. (2) does not yield a closed-form expression; besides, the angular spectrum approach does not even suit for numerical analysis since the involved integrals contain highly oscillating functions. To predict the propagated field, we resort to both the numerical evaluation of Eq. (8) and the perturbation scheme [i.e., Eq. (15)], as the corresponding expression for the field propagating in vacuum is known.

A. Numerical evaluation

In order to numerically compute Eq. (8), we express the field $\mathbf{A}_\perp(\mathbf{r}_\perp,z)$ as a finite two-dimensional Fourier series

$$\mathbf{A}_\perp(\mathbf{r}_\perp,z)=\sum_{n=-N}^{N}\sum_{m=-N}^{N}\mathbf{A}_\perp^{(n,m)}(z)e^{i(2\pi/L)(nx+my)},\tag{22}$$

where L is the size of the squared domain where the field is evaluated. Substituting Eq. (22) into Eq. (8) and exploiting Eq. (A3) of part A of the Appendix, we obtain the Fourier coefficients

$$\mathbf{A}_{\perp}^{(n,m)}(z)=\frac{1}{n^2+m^2}\begin{pmatrix} m^2 & -nm \\ -nm & n^2 \end{pmatrix} \times e^{-[i2\pi^2(n^2+m^2)z/k_0 n_o L^2]}\mathbf{A}_{\perp}^{(n,m)}(0) + \frac{1}{n^2+m^2}\begin{pmatrix} n^2 & nm \\ nm & m^2 \end{pmatrix} \times e^{-[i2\pi^2 n_o(n^2+m^2)z/k_0 n_e^2 L^2]}\mathbf{A}_{\perp}^{(n,m)}(0), \quad (23)$$

where, in the intermediate step, we have substituted each operator with the appropriate eigenvalue. The vector coefficients $\mathbf{A}_{\perp}^{(n,m)}(0)$ are given by the Fourier formula

$$\mathbf{A}_{\perp}^{(n,m)}(0)=\frac{1}{L^2}\int_{-L/2}^{L/2}dx\int_{-L/2}^{L/2}dy\,\mathbf{E}_{\perp}(x,y,0)e^{-i(2\pi/L)(nx+my)} =\frac{2\pi s_x s_y E_0}{L^2}e^{-(2\pi/L^2)(n^2 s_x^2+m^2 s_y^2)}\hat{\mathbf{e}}_x, \quad (24)$$

where Eq. (21) has been taken into account and the integration domain has been replaced with the whole x-y plane. In fact, L is chosen so that the field is neglected on the boundary of the integration domain for every value of z. The choice of N is more critical, since we have to guarantee that all the non-negligible plane waves be taken into account and, roughly speaking, this can be accomplished by choosing $N \gg L/(2\pi\sqrt{s_x^2+s_y^2})$. Equations (24), (23), and (22) allow us to numerically evaluate the field.

We consider an astigmatic Gaussian beam with $\lambda = 0.514$ μm, $s_x = 15$ μm, and $s_y = 6$ μm, propagating in a calcite crystal ($n_o = 1.658$ and $n_e = 1.486$). For each longitudinal propagation distance z, we choose different L and N parameters, so that only the effective region, where the field is not vanishing, is considered. In Fig. 1, we report the level plot of $|E_x|/|E_0|$ at the boundary plane $z=0$ and in Fig. 2 the level plots of $|E_x|/|E_0|$ and $|E_y|/|E_0|$ at $z=2000$ μm, $z=8000$ μm, and $z=20000$ μm. The most important effect of the anisotropy is the growth of the y component of the optical field, as a direct consequence of the coupling between A_x and A_y. The four lobes in the profile of $|A_y|$ can be easily understood by an inspection of Eqs. (7). In fact, for short propagation distances, the field is essentially polarized along the x direction, so that, we can drop the right-hand side of the first of Eqs. (7) and neglect the terms containing $\partial_x^2 A_y$ and $\partial_y^2 A_y$ in the second one. As a consequence, the influence of A_y on A_x is negligible whereas A_x behaves like a pump for A_y by means of the term containing $\partial_{xy}^2 A_x$; this contribution explains the four symmetric lobes in the plot of $|A_y|$, since A_x is bell shaped. As the propagation distance increases, the influence of A_y on A_x increases so that the shape of A_x acquires a more structured profile, as evident from parts (a2) and (a3) of Fig. 2.

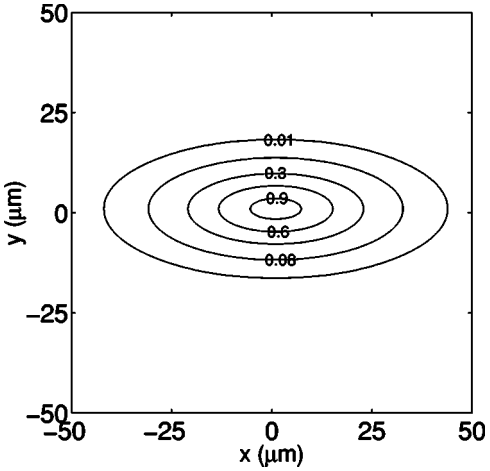

FIG. 1. Level plot for the normalized modulus $|E_x|/|E_0|$ of the astigmatic Gaussian beam with $s_x = 15$ μm, $s_y = 6$ μm at $z=0$ plane.

B. Perturbation scheme

The perturbation scheme of Sec. III A can be efficiently employed in the present case, since the corresponding vacuum-propagating field $\mathbf{A}_{\perp}^{(0)}$ has a closed-form expression [2],

$$\mathbf{A}_{\perp}^{(0)}(\mathbf{r}_{\perp},z)=E_0\left[\left(1+\frac{iz}{k_0 s_x^2}\right)\left(1+\frac{iz}{k_0 s_y^2}\right)\right]^{-1/2} \times\exp\left(-\frac{x^2}{2s_x^2\left(1+\frac{iz}{k_0 s_x^2}\right)} -\frac{y^2}{2s_y^2\left(1+\frac{iz}{k_0 s_y^2}\right)}\right)\hat{\mathbf{e}}_x. \quad (25)$$

By inserting Eq. (25) into Eq. (15), we get the approximate expression for the field inside the crystal, which is valid for $z<z_M=3n_o(s_x^2+s_y^2)/(2\pi\lambda\Delta)$. In the case examined in the preceding subsection it is $z_M \simeq 2000$ μm and in Fig. 3 we report the level plots of $|E_x|/|E_0|$ and $|E_y|/|E_0|$ at $z=1000$ μm and $z=2000$ μm. We computed the mean-square error between the approximated solution and that obtained in the preceding section; for $z=1000$ μm the errors for A_x and A_y components are 0.05% and 2.8%, respectively. For $z=2000$ μm the errors are 0.24% and 9.4% [compare Figs. 2(a1,b1) and Figs. 3(a2,b2)].

C. Experiment

We sketch in Fig. 4 the laboratory setup: the source S is an argon-krypton laser tuned for the $\lambda = 0.514$ μm line and the

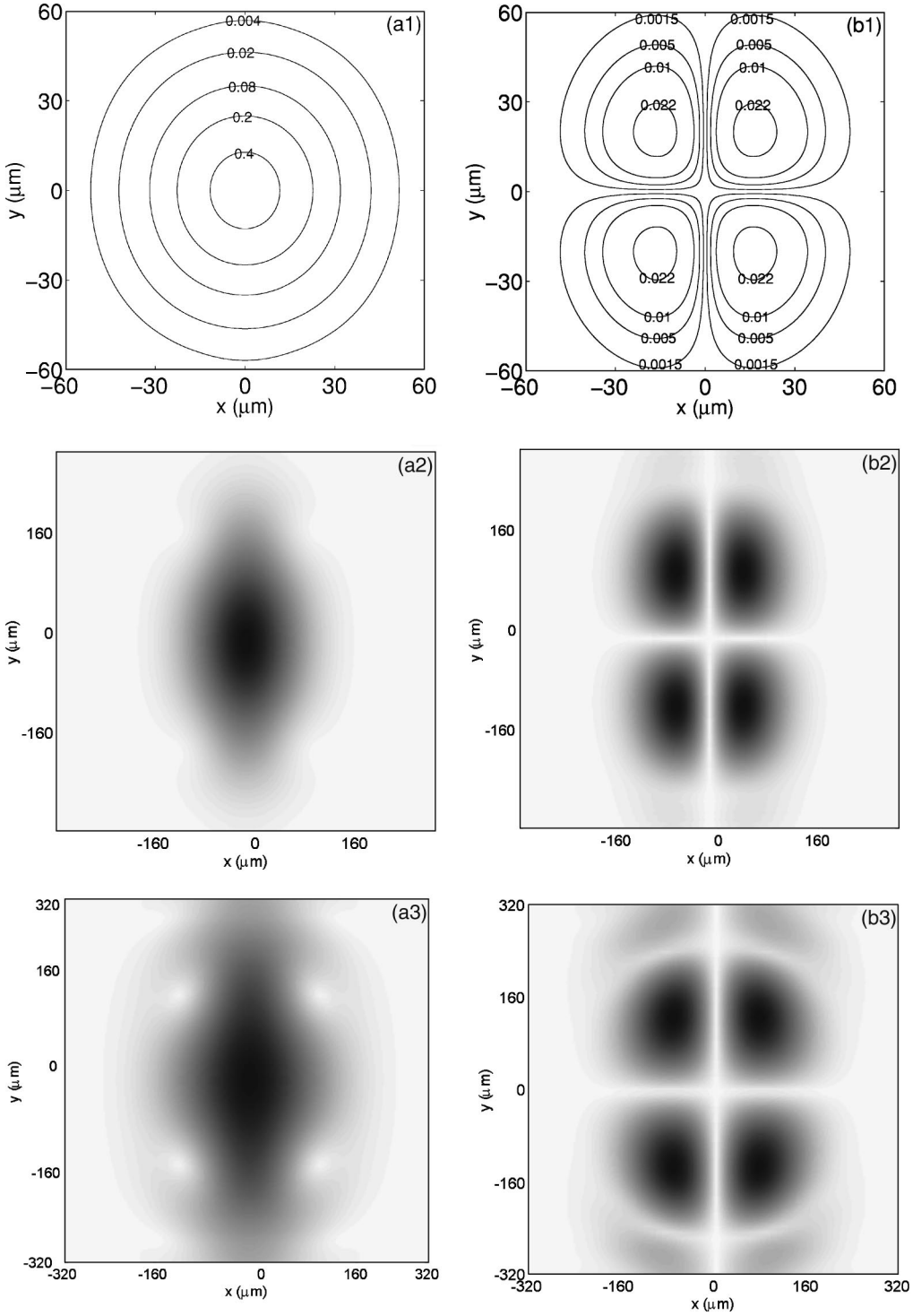

FIG. 2. Level and density plots of the normalized moduli $|E_x|/|E_0|$ (a1) (a2) (a3) and $|E_y|/|E_0|$ (b1) (b2) (b3), obtained by the numerical evaluation, of the astigmatic Gaussian beam ($\lambda = 0.514$ μm, $s_x = 15$ μm, and $s_y = 6$ μm) at the planes $z = 2000$ μm (a1) (b1), $z = 8000$ μm (a2) (b2), $z = 20\,000$ μm (a3) (b3) inside a calcite crystal.

fundamental mode; the output laser beam has a spot size $w_0 = 1$ mm, a divergence $\theta = 1$ mrad, and is linearly polarized. The beam is focused on the entrance facet of a calcite crystal with refractive indices $n_o = 1.658$ and $n_e = 1.486$, cut as a rectangular parallelepiped of size $10 \times 10 \times 20$ mm; the propagation direction of the laser beam coincides with the optical axis, i.e., the longest dimension of the crystal. In order to produce an astigmatic Gaussian beam, we focus the laser beam by means of the two cylindrical lenses L_1 and L_2 of different focal lengths ($f_1 = 20$ cm and $f_2 = 8$ cm, respectively), positioned in order to compound an elliptical waist on the common focus plane. In this way, the resulting ellipse has a ratio 0.4 between the axes and the polarization direction is along the major axis (x axis). This focus plane is then

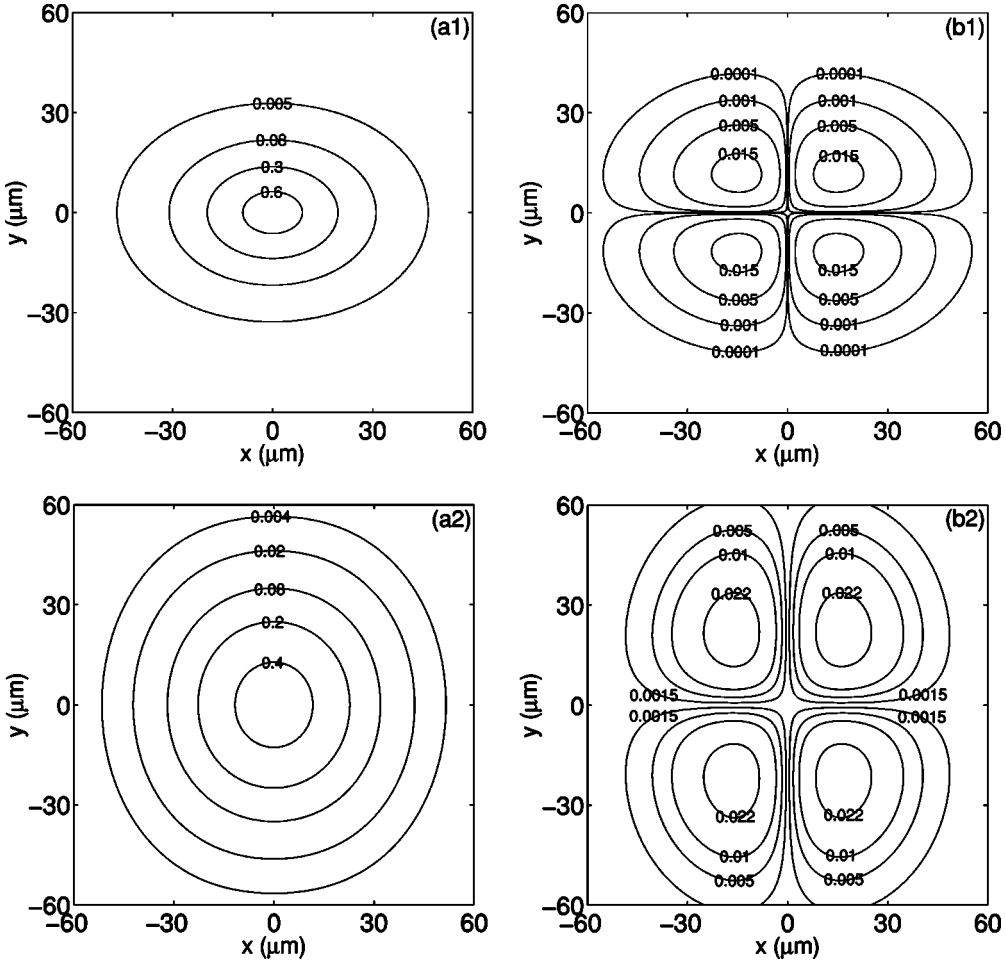

FIG. 3. Level plots of the normalized moduli $|E_x|/|E_0|$ (a1) (a2) and $|E_y|/|E_0|$ (b1) (b2), obtained by the perturbation scheme, of the astigmatic Gaussian beam ($\lambda = 0.514$ μm, $s_x = 15$ μm, and $s_y = 6$ μm) at the planes $z = 1000$ μm (a1) (b1), $z = 2000$ μm (a2) (b2) inside a calcite crystal.

imaged by the lens L_3 on the input facet of the crystal; the lens L_3 and the crystal can be longitudinally shifted in order to obtain an input ellipse of variable dimensions. The crystal length is $D = 20$ mm, and we detect the field only at the output facet. Since we are interested in the detection of the field for various propagation distances, we vary the transverse dimensions of the input waist to vary z. In fact, from Eqs. (2) and Eq. (3), it is easily seen that, if $\mathbf{A}_\perp(\mathbf{r}_\perp, z)$ corresponds to the boundary distribution $\mathbf{E}_\perp(\mathbf{r}_\perp, 0)$, then $\mathbf{A}_\perp(\alpha \mathbf{r}_\perp, \alpha^2 z)$ corresponds to $\mathbf{E}_\perp(\alpha \mathbf{r}_\perp, 0)$; therefore choosing $\alpha = \sqrt{D/z}$ allows us to detect on the output facet the same field that would be detected at distance z with the original dimensions.

The lens L_4 forms a magnified image of either the entrance facet or, by a distance regulation, the exit facet of the crystal on the charge-coupled device detector (3.3 $\times$ 4.4 mm, 576 $\times$ 768 pixel) of a Sony TV camera; the camera is connected to a PC to record, process, and display the images. The rotatable polarizer P allows us to measure the intensity distributions solely due to the x or y components of the electric field.

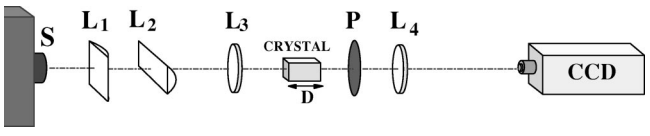

FIG. 4. Experimental setup.

Figure 5 shows the experimental intensity distributions of the two Cartesian components of the optical field, at $z = 8000$ μm and $z = 20\,000$ μm, respectively; for both cases, the theoretical predictions and the experimental results show a very good agreement (see Fig. 2).

V. CONCLUSION

We have introduced an equation describing paraxial propagation along the optical axis of an uniaxial medium. The most important feature of the proposed approach is that it is not based on the standard ordinary-extraordinary decomposition, so that it allows us to investigate some general properties of the propagation which are somehow hidden in the standard angular spectrum approach. The structure of the propagation equation is simple enough to permit us to deduce its formal solution, relating the propagating field to its boundary distribution at $z = 0$. The main consequence is that

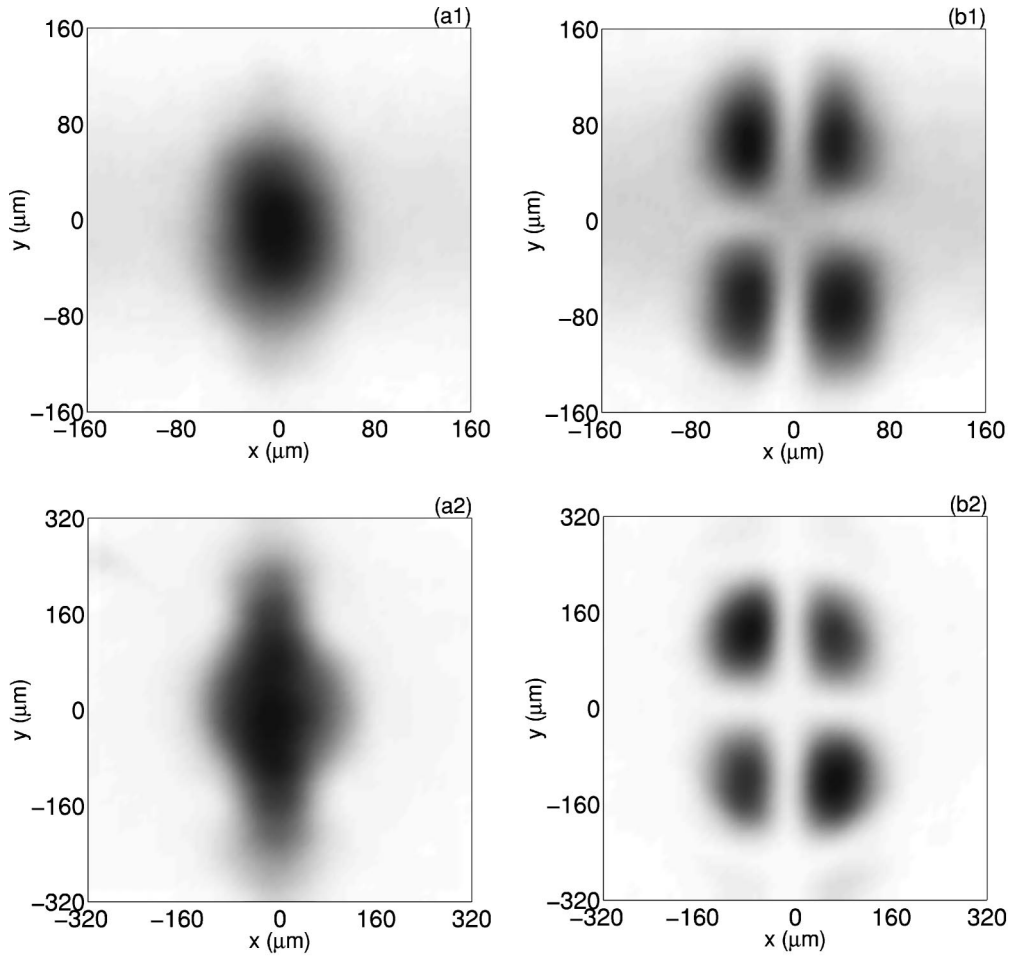

FIG. 5. Experimental intensity distribution of E_x (a1) (a2) and E_y (b1) (b2), of the astigmatic Gaussian beam ($\lambda = 0.514\ \mu$m, $s_x = 15\ \mu$m, and $s_y = 6\ \mu$m) at the planes $z = 8000\ \mu$m (a1) (b1), $z = 20\,000\ \mu$m (a2) (b2) inside a calcite crystal.

we can establish a close connection between the field in the crystal and the corresponding one propagating in vacuum with the same boundary distribution, allowing us to identify the effect of the anisotropy as a perturbation to free propagation. From this conceptual connection, we also derive two analytical techniques for evaluating the field. The first one is embodied in a relation [Eq. (12)] analytically relating the propagating field to that in vacuum, whereas the second one consists in a perturbation scheme which exploits the intrinsic paraxiality of the beam in vacuum. Besides, from the formal solution, we are also able to deduce the expression for the anisotropic propagator. We have chosen the case of the astigmatic Gaussian beam to test some of the results of the proposed approach; then we have implemented a numerical algorithm to evaluate the field from the formal expression. These predictions have been compared with the approximate expression furnished by the perturbation scheme and with experimental results. In all cases the agreement is good.

APPENDIX

A. Derivation of Eq. (12)

In order to obtain from Eq. (11) a less formal expression, let us consider the operator $\hat{\mathbf{D}}$ and its powers series definition

$$\hat{\mathbf{D}}(z) = e^{(iz\Delta/2k_0 n_o)\hat{\mathbf{T}}} = 1 + \sum_{n=1}^{\infty} \frac{1}{n!} \left(\frac{iz\Delta}{2k_0 n_o} \right)^n \hat{\mathbf{T}}^n. \quad \text{(A1)}$$

Because of the structure of the operator $\hat{\mathbf{T}}$ it is easy to work out $\hat{\mathbf{T}}^n$, that is,

$$\hat{\mathbf{T}}^n = \left[\begin{pmatrix} \partial_x \\ \partial_y \end{pmatrix} (\partial_x \ \partial_y) \right]^n = \begin{pmatrix} \partial_x \\ \partial_y \end{pmatrix} (\nabla_\perp^2)^{n-1} (\partial_x \ \partial_y) = \hat{\mathbf{T}} (\nabla_\perp^2)^{n-1}, \quad \text{(A2)}$$

valid for $n \geqslant 1$. This relation allows us to rewrite Eq. (A1), after some operatorial manipulation, as

$$\hat{\mathbf{D}}(z) = (\nabla_\perp^2)^{-1} [(\nabla_\perp^2 - \hat{\mathbf{T}}) + \hat{\mathbf{T}} e^{(iz\Delta/2k_0 n_o)\nabla_\perp^2}]. \quad \text{(A3)}$$

Inserting this expression for the dressing operator $\hat{\mathbf{D}}(z)$ into Eq. (11), we obtain the relation

$$\mathbf{A}_\perp(\mathbf{r}_\perp,z)=(\nabla_\perp^2)^{-1}\left[(\nabla_\perp^2-\hat{\mathbf{T}})\mathbf{A}_\perp^{(0)}\left(\mathbf{r}_\perp,\frac{z}{n_o}\right)+\hat{\mathbf{T}}\cdot\mathbf{A}_\perp^{(0)}\left(\mathbf{r}_\perp,\frac{n_o z}{n_e^2}\right)\right], \tag{A4}$$

where we have exploited the propagation property of the vacuum field,

$$e^{(iz_2/2k_0)\nabla_\perp^2}\mathbf{A}_\perp^{(0)}(\mathbf{r}_\perp,z_1)=\mathbf{A}_\perp^{(0)}(\mathbf{r}_\perp,z_1+z_2). \tag{A5}$$

Applying the operator $\nabla_\perp^2$ to both members in Eq. (A4), we obtain

$$\nabla_\perp^2\mathbf{A}_\perp(\mathbf{r}_\perp,z)=\begin{pmatrix}\partial_y^2 & -\partial_{xy}^2\\ -\partial_{xy}^2 & \partial_x^2\end{pmatrix}\mathbf{A}_\perp^{(0)}\left(\mathbf{r}_\perp,\frac{z}{n_o}\right)+\begin{pmatrix}\partial_x^2 & \partial_{xy}^2\\ \partial_{xy}^2 & \partial_y^2\end{pmatrix}\mathbf{A}_\perp^{(0)}\left(\mathbf{r}_\perp,\frac{n_o z}{n_e^2}\right), \tag{A6}$$

which are two two-dimensional Poisson equations for A_x and A_y, since the right-hand side is supposed to be known. Therefore, assuming that the field $\mathbf{A}_\perp$ vanishes at infinity on the transverse plane, Eq. (A6) can be straightforwardly solved, yielding

$$\mathbf{A}_\perp(\mathbf{r}_\perp,z)=\frac{1}{2\pi}\int d^2\mathbf{r}'_\perp\ln|\mathbf{r}_\perp-\mathbf{r}'_\perp|\left[\begin{pmatrix}\partial_y'^2 & -\partial_{x'y'}^2\\ \partial_{x'y'}^2 & \partial_x'^2\end{pmatrix}\mathbf{A}_\perp^{(0)}\left(\mathbf{r}'_\perp,\frac{z}{n_o}\right)+\begin{pmatrix}\partial_x'^2 & \partial_{x'y'}^2\\ \partial_{x'y'}^2 & \partial_y'2\end{pmatrix}\mathbf{A}_\perp^{(0)}\left(\mathbf{r}'_\perp,\frac{n_o z}{n_e^2}\right)\right]. \tag{A7}$$

Splitting this equation into the sum of two integrals, then integrating by parts twice with respect to both x' and y' and exploiting the symmetry properties of $|\mathbf{r}_\perp-\mathbf{r}'_\perp|$, we obtain Eq. (12).

B. Evaluation of the ordinary and extraordinary propagators

Let us introduce polar coordinates, both for $\mathbf{R}=X\hat{\mathbf{e}}_x+Y\hat{\mathbf{e}}_y=\mathbf{r}_\perp-\mathbf{r}'_\perp$ and for $\mathbf{k}_\perp$,

$$X=R\cos\varphi,\quad k_x=k\cos\theta,$$
$$Y=R\sin\varphi,\quad k_y=k\sin\theta, \tag{A8}$$

which allow us to rewrite the ordinary propagator of Eq. (18) as

$$\mathbf{G}_o(\mathbf{R})=\frac{1}{(2\pi)^2}\int_0^\infty dkke^{-(iz/2k_0n_o)k^2}\int_0^{2\pi}d\theta e^{ikR\cos(\theta-\varphi)}\times\begin{pmatrix}\sin^2\theta & -\cos\theta\sin\theta\\ -\cos\theta\sin\theta & \cos^2\theta\end{pmatrix}. \tag{A9}$$

The integral on θ can be evaluated by means of the well-known Anger-Jacobi relation

$$e^{ikR\cos(\theta-\varphi)}=\sum_{n=-\infty}^{+\infty}i^nJ_n(kR)e^{in(\theta-\varphi)}, \tag{A10}$$

where $J_n(\xi)$ is the Bessel function of the first kind and order n. Inserting Eq. (A10) into Eq. (A9), the integrals on θ become trivial, thus getting

$$\mathbf{G}_o(\mathbf{R})=\begin{pmatrix}1 & 0\\ 0 & 1\end{pmatrix}\frac{1}{4\pi}\int_0^\infty dkke^{-(iz/2k_0n_o)k^2}J_0(kR)+\begin{pmatrix}\cos2\varphi & \sin2\varphi\\ \sin2\varphi & -\cos2\varphi\end{pmatrix}\times\frac{1}{4\pi}\int_0^\infty dkke^{-(iz/2k_0n_o)k^2}J_2(kR). \tag{A11}$$

The integrals on k can be analytically evaluated [27], so that we have

$$\mathbf{G}_o(\mathbf{R})=\frac{k_0n_o}{4\pi iz}e^{-(k_0n_o/2iz)R^2}\begin{pmatrix}1 & 0\\ 0 & 1\end{pmatrix}-\left[\frac{k_0n_o}{4\pi iz}e^{-(k_0n_o/2iz)R^2}-\frac{1-e^{-(k_0n_o/2iz)R^2}}{2\pi R^2}\right]\begin{pmatrix}\cos2\varphi & \sin2\varphi\\ \sin2\varphi & -\cos2\varphi\end{pmatrix}. \tag{A12}$$

Expressing the trigonometric functions by means of X and Y we obtain the ordinary propagator of Eq. (19). An analogous calculation yields the extraordinary propagator.

[1] M. Born and E. Wolf, *Principles of Optics* (Pergamon Press, Oxford, 1999).

[2] A. Yariv and P. Yeh, *Optical Waves in Crystals* (Wiley, New York, 1984).

[3] H. Chen, *Theory of Electromagnetic Waves* (McGraw-Hill, New York, 1983).

[4] T. Sonoda and S. Kozaki, Electron. Commun. Jpn. **72**, 95 (1989).

[5] D. Jiang and J. Stamnes, Opt. Commun. **163**, 55 (1999).
[6] D. Jiang and J. Stamnes, Opt. Commun. **174**, 321 (2000).
[7] J. Stamnes and V. Dhayalan, J. Opt. Soc. Am. A **18**, 1662 (2001).
[8] C.L. Xu, W.P. Huang, J. Chrostowski, and S.K. Chaudhuri, J. Lightwave Technol. **12**, 1926 (1994).
[9] J.F. Mosino, O.B. Garcia, A. Starodumov, L.A. Diaz-Torres, M.A. Meneses-Nava, and J.T. Vega-Duran, Opt. Commun. **173**, 57 (2000).
[10] R. Martinez-Herrero, J.M. Movilla, and P.M. Mejias, J. Opt. Soc. Am. A **18**, 2009 (2001).
[11] U. Hempelmann, H. Herrmann, G. Mrozynski, V. Reimann, and W. Sohler, J. Light Technol. **13**, 1750 (1995).
[12] R. Wolfe, R. A. Lieberman, V. J. Fratello, R. E. Scotti, and N. Kopylov, Appl. Phys. Lett. **56**, 426 (1990).
[13] O. Zhuromoskyy, M. Lohmeyer, N. Bahlmann, H. Dotsch, P. Hertel, and A. Popkov, J. Light Technol. **17**, 1200 (1999).
[14] J. Stamnes and G.C. Sherman, J. Opt. Soc. Am. **66**, 780 (1976).
[15] J.A. Fleck and M. Feit, J. Opt. Soc. Am. **73**, 920 (1983).
[16] M. Trippenbach and Y. Band, J. Opt. Soc. Am. B **13**, 1403 (1996).
[17] Y. Band and M. Trippenbach, Phys. Rev. Lett. **76**, 1457 (1996).
[18] C. Radzewicz, J. Krasinski, M. la Grone, M. Trippenbach, and Y. Band, J. Opt. Soc. Am. B **14**, 420 (1997).
[19] M. Trippenbach, T. Scott, and Y. Band, Opt. Lett. **22**, 579 (1997).
[20] A. Ciattoni, B. Crosignani, and P. Di Porto, J. Opt. Soc. Am. A **18**, 1656 (2001).
[21] A. Ciattoni, G. Cincotti, C. Palma, and H. Weber, J. Opt. Soc. Am. A **19**, 1894 (2002).
[22] G. Cincotti, A. Ciattoni, and C. Palma, J. Opt. Soc. Am. A **19**, 1680 (2002).
[23] A. Ciattoni, G. Cincotti, and C. Palma, Opt. Commun. **195**, 55 (2001).
[24] A. Ciattoni, G. Cincotti, and C. Palma, J. Opt. Soc. Am. A **19**, 792 (2002).
[25] G. Cincotti, A. Ciattoni, and C. Palma, IEEE J. Quantum Electron. **12**, 1517 (2001).
[26] J. Goodman, *Introduction to Fourier Optics* (University of California Press, Berkeley, 1966).
[27] A. Prudnikov, Y. Brychkov, and O. Marichev, *Integrals and Series* (Gordon and Breach Science Publishers, Amsterdam, 1986).